Lack of vacuolar proton ATPase association with the cytoskeleton in osteoclasts of osteosclerotic (*oc/oc*) mice

Ichiro Nakamura[a,c], Naoyuki Takahashi[a], Nobuyuki Udagawa[a], Yoshinori Moriyama[b], Takahide Kurokawa[c], Eijiro Jimi[a], Takahisa Sasaki[a], Tatsuo Suda[a,*]

[a] *Departments of Biochemistry and Oral Anatomy, School of Dentistry, Showa University, 1-5-8 Hatanodai, Shinagawa-ku, Tokyo 142, Japan*
[b] *Division of Molecular Biology, Graduate School of Gene Science, Hiroshima University, Mukaishima, Hiroshima 722, Japan*
[c] *Department of Orthopedics, School of Medicine, University of Tokyo, 7-3-1 Hongo, Bunkyo-ku, Tokyo 113, Japan*

Received 1 November 1996; revised version received 5 December 1996

Abstract We examined the pathogenetic mechanism underlying the lack of bone resorption in osteosclerotic *oc/oc* mice. An immunoelectron microscopic analysis revealed that in the osteoclasts of these mice, no ruffled borders formed, and that vacuolar H^+-ATPase (V-ATPase) was present throughout the cytoplasm but not on the apical membranes. The activity of V-ATPase in *oc/oc* mice was similar to that in normal mice. In normal spleen cell-derived osteoclast-like cells (OCLs), immunoreactivity for V-ATPase was detected in association with Triton X-100-insoluble cellular structure, but not in *oc/oc* spleen cell-derived OCLs. Moreover, in renal proximal convoluted tubules of *oc/oc* mice, the basal striation did not form. These results suggest that osteosclerosis in *oc/oc* mice is possibly due to the dissociation of V-ATPase and cytoskeleton in osteoclasts.

Key words: Osteosclerosis; *oc/oc*; Vacuolar proton ATPase; Ruffled border; Renal proximal convoluted tubule

1. Introduction

Osteoclasts are primary bone-resorbing cells, which exhibit a highly polarized cytoplasmic organization, the ruffled border, on which vacuolar H^+-ATPase (V-ATPase) is localized in a high density [1]. V-ATPase pumps protons out into resorption lacunae, where bone mineral is dissolved by acidic pH [1,2]. Osteopetrosis is an inherited disease characterized by an increase in bone mass due to reduced bone resorption [3]. In mice, there are four genetically distinct osteopetrotic mutations: *gl/gl* which is characterized by gray hair and is lethal, *op/op* characterized by osteopetrotic bone lesions [4], *mi/mi* characterized by microphthalmia [5], and *oc/oc* characterized by osteosclerotic bone lesions. Although for each type of osteopetrosis the mutations exist on different chromosomes, all types of osteopetrosis have similar radiographic features. These include a marked increase in skeletal density and narrowing of the marrow cavity.

The osteosclerotic *oc/oc* mutation is lethal, typically causing death within 3 weeks of birth [3]. In *oc/oc* mice, small and numerous osteoclasts are recognized in bone tissues, but they do not appear to be functionally active, resulting in no bone marrow cavities [6]. It was reported that transplantation of hemopoietic cells into *oc/oc* mice failed to cure bone disorders [7]. We have developed a co-culture system of murine spleen cells and osteoblastic cells, in which osteoclast-like multinucleated cells (OCLs) are formed in response to 1α,25-dihydroxyvitamin D_3 (1α,25$(OH)_2D_3$) [8]. Using this co-culture system, we found that osteoblastic cells obtained from *oc/oc* mice were capable of supporting osteoclast development from normal spleen cells, and that *oc/oc* spleen cells could also differentiate into OCLs in co-cultures with normal osteoblastic cells [9]. These *oc/oc* spleen cell-derived OCLs strongly expressed proteins such as carbonic anhydrase II, vitronectin receptor ($\alpha_V\beta_3$ integrin), V-ATPase, and $p60^{c-src}$, but they formed neither ruffled borders nor resorption pits on dentine slices [9,10]. These results clearly indicate that the failure of bone resorption in *oc/oc* mice is due to a defect in osteoclast progenitors, rather than in the osteoblastic cells which provide the local microenvironment for osteoclastogenesis. In the present study, we examined the detailed pathogenesis of osteosclerosis in *oc/oc* mice. We report here lack of V-ATPase association with detergent-resistant cellular structure, probably the cytoskeleton, in OCLs of *oc/oc* mice, suggesting that dissociation of V-ATPase and cytoskeleton may correlate with osteopetrosis in *oc/oc* mice.

2. Materials and methods

2.1. Animals

(C57BL/6J×C3HeB/FeJ) F1-oc/+ parent mice were obtained from the Jackson Laboratory (Bar Harbor, ME). A quarter of their littermates are expected to be osteosclerotic (*oc/oc*). The *oc/oc* homozygotes were radiologically distinguished at birth from phenotypically normal, +/? siblings.

2.2. Preparation of osteoclast-like multinucleated cells

Spleen cells from either *oc/oc* or +/? littermates were co-cultured with normal osteoblastic cells from calvaria of newborn ddY mice in a-MEM containing 10% FBS and 10 nM 1α,25$(OH)_2D_3$ on 60-mm culture dishes precoated with 2 ml of 0.2% collagen gel matrix (Nitta Gelatin Co., Osaka, Japan) [9,11]. OCLs were formed within 8 days of culture, and were released from the dishes by treatment with 2 ml of 0.2% collagenase (Wako Pure Chemical Co., Osaka), before being collected by centrifugation at 250×*g* for 5 min.

2.3. Association of V-ATPase with detergent-resistant cellular structure

Association of V-ATPase with detergent-resistant cellular structure was examined as reported previously with a slight modification [12,13]. In short, after OCL preparations were cultured for 2 h on culture plates, cells were treated with Triton X-100 in PBS for 10 min at various concentrations, washed three times with PBS, and fixed with methanol-acetone (50:50, v/v) for 10 min. Then, some cells were incubated with polyclonal antibody against the 72 kDa subunit of V-ATPase [14] or against carbonic anhydrase II [15]. The bound antibodies were visualized with biotinylated second antibodies, streptavidin-conjugated peroxidase, and a DAB substrate kit (Histofine, Nichirei Co., Tokyo, Japan). Others were stained for tartrate-resistant acid phosphatase (TRAP), a typical marker enzyme of osteoclasts, as described previously [8].

2.4. Measurement of proton transport

Brain synaptic vesicle fraction from either *oc/oc* mice or control ddY mice was prepared by the published procedure [16]. ATP-de-

*Corresponding author. Fax: (81) (3) 3784-5555.

PII S0014-5793(96)01454-8

pendent H^+ transport was measured by assay of quenching of acridine orange fluorescence in a Hitachi F-3000 fluorescence spectrophotometer with excitation and emission wave lengths of 492 and 540 nm, respectively. The standard assay was carried out in 20 mM MOPS-Tris, pH 7.0, containing 0.1 M KCl, 2 mM acridine orange and 80 mg of protein derived from the cerebellum of either *oc/oc* or control ddY mice, and was started by addition of a mixture of 0.5 mM ATP and 0.5 mM $MgCl_2$. When necessary, concanamycin B, a specific inhibitor for V-ATPase [17], suspended in dimethylsulfoxide was involved in the assay buffer.

2.5. Electron microscopic examination

Under anesthesia with sodium pentobarbital, 2-week-old *oc/oc* or +/? mice were fixed by perfusion with a mixture of 4% formaldehyde and 0.1% glutaraldehyde in 0.1 M sodium cacodylate buffer (pH 7.3), and the dissected humeri were demineralized in 10% EDTA. Their metaphyses were embedded in medium grade LR gold resin (London Resin Co. Ltd., Basingstoke, UK) and polymerized at −20°C under ultraviolet rays. Ultrathin sections were mounted on formvar-coated nickel grids and treated with 10% BSA in PBS for 30 min to block the non-specific binding of antiserum. The sections were then incubated overnight at 4°C with anti-V-ATPase antibody [14], followed by incubation for 1 h with goat anti-rabbit IgG conjugated with 10 nm colloidal gold particles (BioCell Research Laboratories, Cardiff, UK). After rinsing with PBS and distilled water, the sections were stained with 2% uranyl acetate and examined in a Hitachi HU-12A electron microscope.

To observe the ultrastructure of kidney of *oc/oc* mice, mice were fixed by perfusion with a mixture of 2.5% glutaraldehyde in 0.1 M sodium cacodylate buffer (pH 7.3). The dissected kidneys were post-fixed with 1% osmium tetroxide, block-stained with 1% uranyl acetate, dehydrated through a graded ethanol series, and embedded in Quetol 812 (Nisshin EM, Tokyo). Ultrathin sections were stained with uranyl acetate and lead citrate, and examined as described above.

3. Results and Discussion

It has been reported that osteoclasts in *oc/oc* mice lack ruffled borders [6,9]. Thus, we first examined the subcellular localization of V-ATPase in osteoclasts of *oc/oc* mice by immunoelectron microscopy. In normal osteoclasts, specific immunogold labeling was detected along the ruffled border membranes (Fig. 1a). In *oc/oc* osteoclasts, however, specific immunolabeling of V-ATPase was detected not along the apical membranes facing the bone surfaces, but in the cytoplasm (Fig. 1b). As to the distribution of V-ATPase in cytosolic compartment, there was no appreciable difference between normal and *oc/oc* osteoclasts. In both osteoclasts, V-ATPase was present similarly on intracellular vacuoles and rough endoplasmic reticulum (data not shown). The only difference between normal and *oc/oc* osteoclasts lay in the localization of V-ATPase in ruffled border (apical) membranes.

The density of V-ATPase appeared to be higher along ruffled border membranes of normal osteoclasts than apical membranes of *oc/oc* osteoclasts. However, immunostaining for V-ATPase by light microscopy revealed that *oc/oc* spleen cell-derived OCLs expressed V-ATPase as abundantly as normal OCLs (Fig. 3c,d). Moreover, in order to determine whether there is a defect in the V-ATPase activity in *oc/oc* mice, we prepared membrane vesicles from the cerebellum, and measured the ability for V-ATPase to transport H^+ by an ATP-dependent mechanism. V-ATPase derived from *oc/oc* cerebellum had similar ability to transport H^+ to that from normal cerebellum (Fig. 2). Also when we used membrane vesicles derived from OCLs, we could not detect any appreciable differences in the activity of V-ATPase between normal and *oc/oc* mice (data not shown). These results suggest that the defect of bone-resorbing activity of *oc/oc* osteoclasts is due to the subcellular localization of V-ATPase, but to neither its expression level nor activity.

We next examined the association of V-ATPase with the cytoskeleton of osteoclasts, using in vitro culture systems. TRAP, carbonic anhydrase II, and V-ATPase, which are typical marker enzymes for osteoclasts, were present in not only normal spleen cell-derived OCLs (Fig. 3a-c) but also *oc/oc* spleen cell-derived OCLs (Fig. 3d). When non-immune serum were used as the first antibody, no specific immunolabeling was detected (data not shown). When normal OCLs were treated with 0.05% Triton X-100 to perforate plasma membranes, enzyme reactivity of TRAP and immunoreactivity for carbonic anhydrase II were not detected, suggesting that these enzymes are not associated with detergent-resistant structure but present in the cytosolic compartment (Fig. 3e,f). Previous reports indicated that this detergent-resistant subcellular structure consisted largely of cytoskeleton [12,13]. We also confirmed by scanning electron microscopy that Triton-insoluble subcellular structure still remained on the surface of culture plates (data not shown). However, immunoreactivity for V-ATPase was detected in the Triton-insoluble structure, even when cells were treated with 0.15% Triton X-100 (Fig. 3g, arrowheads), suggesting that V-ATPase was associated with detergent-resistant subcellular structure, probably the cytoskeleton of osteoclasts. When *oc/oc* spleen cell-derived OCLs were treated with 0.05% Triton-X 100, enzyme reactivity of TRAP and immunoreactivity for carbonic anhydrase II were not detected as well (data not shown). On the other hand, interestingly, no immunoreactivity for V-ATPase was detected in *oc/oc* OCLs treated with 0.05% Triton-X 100 (Fig. 3h), suggesting the failure in the association of V-ATPase with detergent-resistant subcellular structure in *oc/oc* osteoclasts. All these findings led us to the hypothesis that, in *oc/oc* mice, there may exist a defect of a molecule which directly or indirectly connects V-ATPase with the cytoskeleton, resulting in the disorder of intracellular localization of V-ATPase.

The relationship between ruffled border formation and intracellular localization of V-ATPase is not well established. Sorting of V-ATPase onto the apical membranes may cause the membrane ruffling, resulting in ruffled border formation, while ruffled border formation may be necessary for the V-ATPase sorting. However, V-ATPase is present along not only ruffled borders but also intracellular associated vacuoles near the ruffled borders [18]. These findings together with the present study suggest that sorting of V-ATPase with membrane vacuoles onto ruffled borders may simultaneously supply membrane components to the apical membranes, leading to ruffled border formation. Normalization of the intracellular

→

Fig. 1. Immunoelectron microscopic localization of V-ATPase in osteoclasts in *oc/oc* mice. Metaphyseal sections of humeri of either *oc/oc* (b) or +/? mice (a) were incubated with polyclonal antibody against the 72 kDa subunit of V-ATPase and processed for immunocytochemical localization of V-ATPase with 10 nm colloidal gold particles. In normal osteoclasts, intense immunolabeling is visible along the ruffled border membranes (a). In *oc/oc* osteoclasts, specific labeling is detected not along the apical membranes facing bone surfaces, but in the cytoplasm (b). RB, ruffled border. Bars = 0.5 μm.

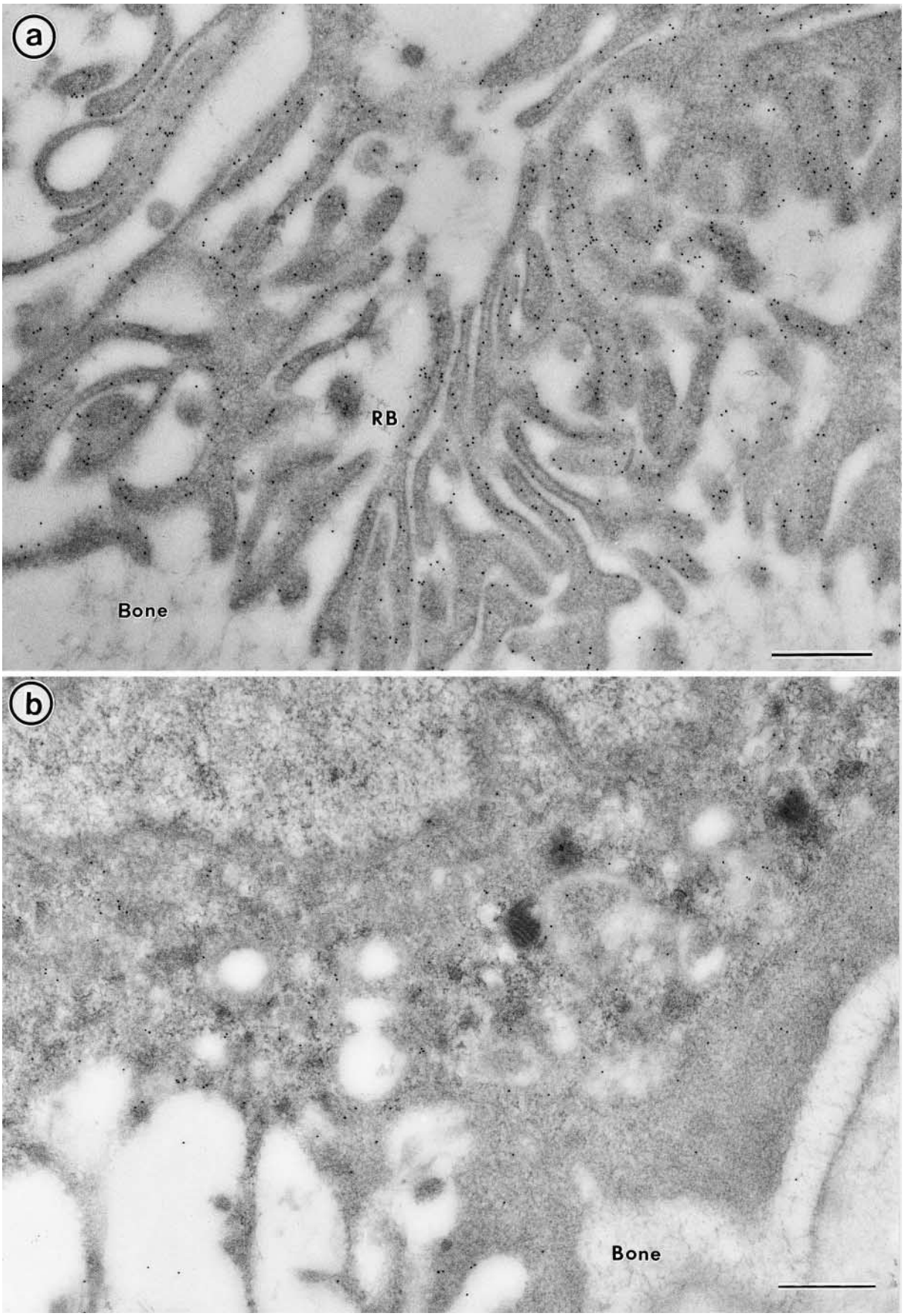
a
RB
Bone
b
Bone

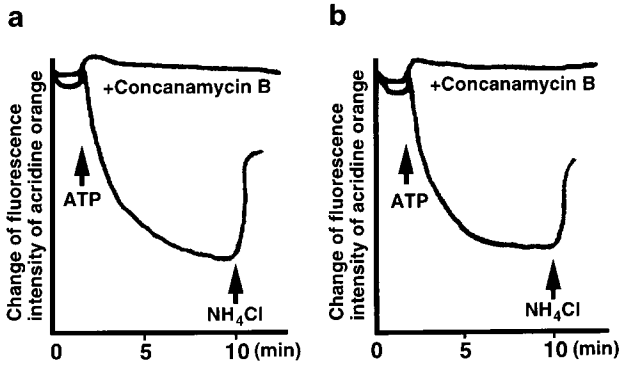

Fig. 2. ATP-dependent H^+ transport in *oc/oc* mice. Membrane vesicles prepared from cerebellum (80 mg of protein) of either *oc/oc* (b) or ddY control mice (a) were assayed with acridine orange. Changes of fluorescence intensity of acridine orange (5 mM) (excitation, 492 nm; emission, 540 nm) were monitored in the presence of 0.5 mM $MgCl_2$ and 0.5 mM ATP with or without concanamycin B (50 nM). ATP and NH_4Cl (10 mM) were added as indicated.

localization of V-ATPase may lead to ruffled border formation in *oc/oc* osteoclasts, then to the rescue of osteopetrosis in *oc/oc* mice.

Finally, we examined the ultrastructure of renal proximal convoluted tubules in *oc/oc* mice, because osteoclasts and proximal convoluted tubules of kidney exhibit a highly polarized cytoplasmic organization consisting of numerous deep membrane invaginations, that is, ruffled borders and basal striations, respectively, and abundantly express V-ATPase with polarity. Electron microscopic examination revealed that numerous electron dense bodies were recognized in the cytoplasm of proximal convoluted tubules and that the basal striation, a crucial area for the transport of ions, did not form (Fig. 4b). These results indicate that in *oc/oc* mice, a defect exists not only in osteoclastic bone resorption but also in renal function. This disorder in proximal convoluted tubules of kidney may result in the early death (about 3 weeks after birth) of *oc/oc* mutants. We could not find any definite ultrastructural disorders in other organs such as the stomach, small intestine, or cerebellum (data not shown).

Very recently, Beier et al. have reported that a novel putative transporter is lacking in *oc/oc* mice, causing osteopetrosis [19]. According to their report, this transporter, a homologue of a family of 12-transmembrane domain proteins, is likely to be expressed only in kidney and osteoclasts. Taken together with our present study, there is a coincidence in the possibility that in *oc/oc* mice, a defect in the function of osteoclasts and kidney exists. However, it is still not known how this novel

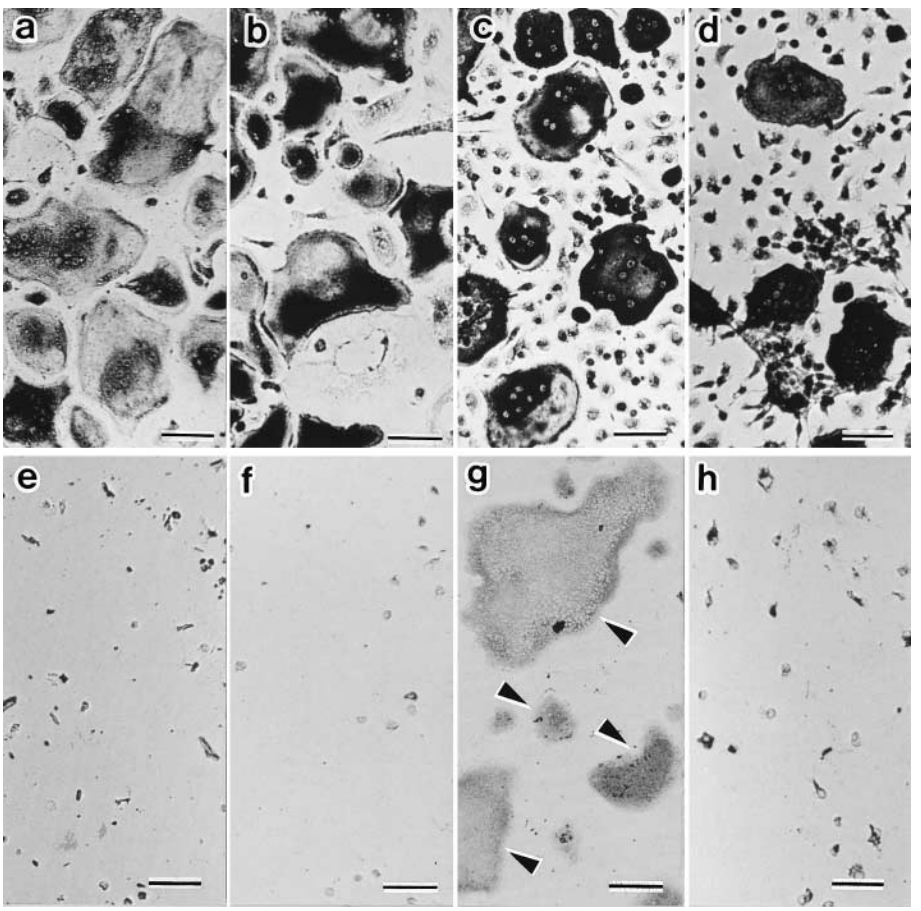

Fig. 3. Association of V-ATPase with detergent-resistant cellular structure in *oc/oc* OCLs. After normal spleen cell-derived OCLs (a–c, e–g) or *oc/oc* spleen cell-derived OCLs (d, h) were cultured for 2 h on culture plates, cells were treated with 0% (a–d), 0.05% (e, f, h) or 0.15% (g) Triton X-100 in PBS for 10 min, washed three times with PBS, and fixed with methanol-acetone (50:50, v/v) for 10 min. Some cells were immunostained with polyclonal antibody against the 72 kDa subunit of V-ATPase (c, d, g, h) or against carbonic anhydrase II (b, f). Others were stained for tartrate-resistant acid phosphatase (a, e). Note that immunoreactivity for V-ATPase is detected in normal OCLs (g, arrowheads) but not in *oc/oc* OCLs (h), when cells were treated with Triton-X 100. Bars = 50 μm.

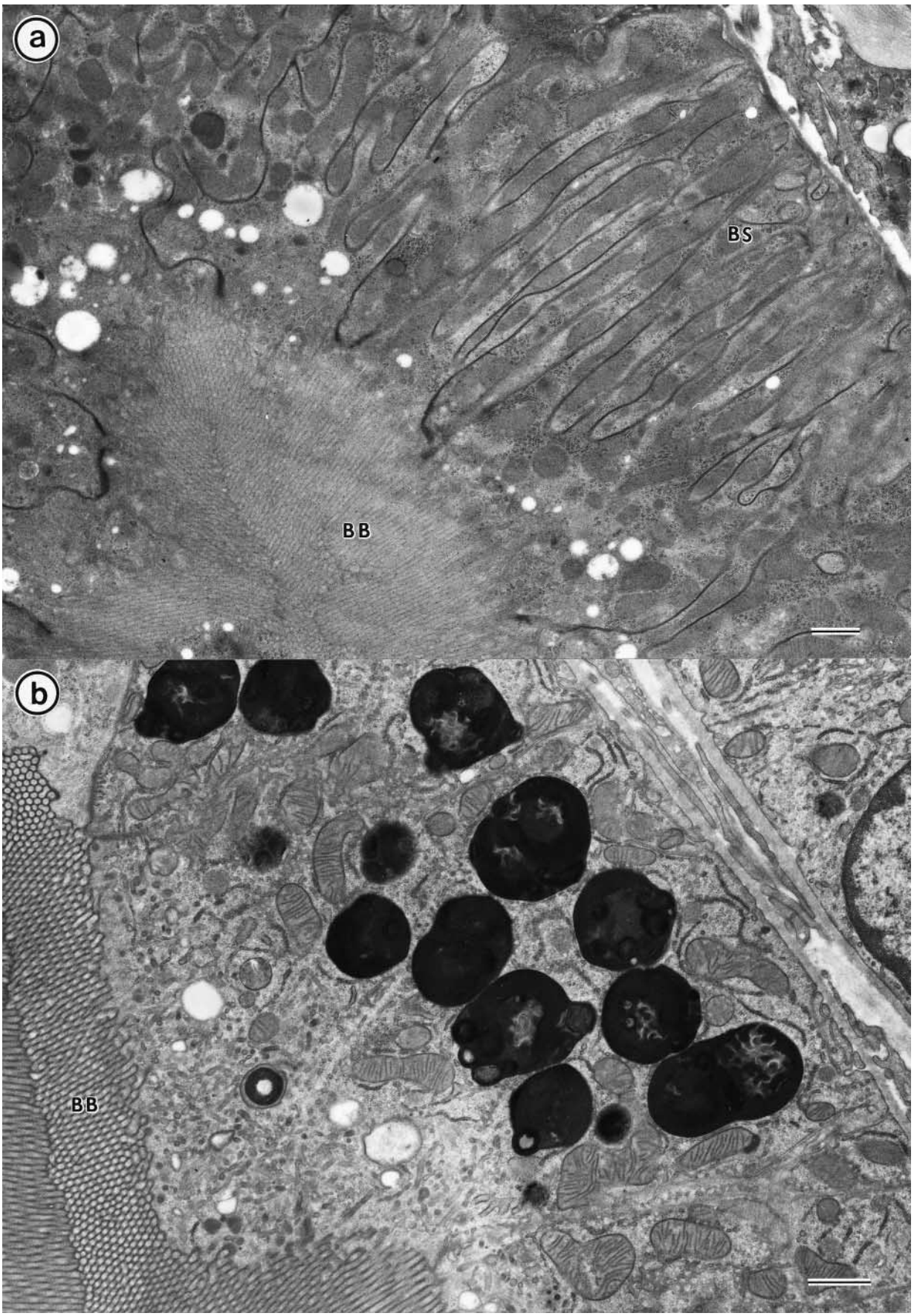

Fig. 4. An electron micrograph of renal proximal convoluted tubules in normal (a) and *oc/oc* mice (b). Note that numerous electron dense bodies are recognized in the cytoplasm of proximal convoluted tubules of *oc/oc* kidney and that no basal striations form. BB, brush border; BS, basal striation. Bars = 1 μm.

transporter is involved in the intracellular localization of V-ATPase and its association with cytoskeleton. Further studies are required to determine a more detailed mechanism of osteosclerosis in *oc/oc* mice and the function of this novel transporter in osteoclasts.

Acknowledgements: We thank Dr. Ryu-ichi Nishinakamura (University of Tokyo) for his valuable advice, and Dr. H. Kalervo Väänänen for the gift of anti-carbonic anhydrase II antibody. This study was supported in part by Grants-in-Aid (08672088, 07557118 and 07457441) from the Ministry of Science, Education and Culture of Japan.

References

[1] Blair, H.C., Teitelbaum, S.L., Ghiselli, R. and Gluck, S. (1989) Science 245, 855–857.
[2] Väänänen, H.K., Karhukorpi, E.K., Sundquist, K., Wallmark, B., Roininen, I., Hentunen, T., Tuukkanen, J. and Lakkakorpi, P. (1990) J. Cell Biol. 111, 1305–1311.
[3] Marks, Jr. S.C. (1989) Am. J. Med. Genet. 34, 43–54.
[4] Yoshida, H., Hayashi, S., Kunisada, T., Ogawa, M., Nishikawa, S., Okamura, H., Sudo, T., Shultz, L.D. and Nishikawa, S. (1990) Nature 345, 442–444.
[5] Hodgkinson, C.A., Moore, K.J., Nakayama, A., Steingrimsson, E., Copeland, N.G., Jenkins, N.A. and Arnheiter, H. (1993) Cell 74, 395–404.
[6] Seifert, M.F. and Marks, Jr. S.C. (1985) Am. J. Anat. 172, 141–153.
[7] Seifert, M.F. and Marks, Jr. S.C. (1987) Tissue Cell 19, 29–37.
[8] Takahashi, N., Akatsu, T., Udagawa, N., Sasaki, T., Yamaguchi A., Moseley, J.M., Martin, T.J. and Suda, T. (1988) Endocrinology 123, 2600–2602.
[9] Udagawa, N., Sasaki, T., Akatsu, T., Takahashi, N., Tanaka, S., Tamura, T., Tanaka, H. and Suda, T. (1992) Biochem. Biophys. Res. Commun. 184, 67–72.
[10] Udagawa, N., Takahashi, N., Sasaki, T., Akatsu, T., Tanaka, S., Tamura, T., Tanaka, H., Moriyama, Y., Futai, M., Kanehisa, J., Väänänen, K. and Suda, T. (1992) in: Calcium Regulating Hormones and Bone Metabolism (Cohn, D.V., Gennari, C. and Tashjian, Jr. A.H., Eds.), pp. 151–156, Elsevier, Amsterdam.
[11] Akatsu, T., Tamura, T., Takahashi, N., Udagawa, N., Tanaka, S., Sasaki, T., Yamaguchi, A., Nagata, N. and Suda, T. (1992) J. Bone Mineral Res. 7, 1297–1306.
[12] Ben-Ze'ev, A., Duerr, A., Solomon, F. and Penman, S. (1979) Cell 17, 859–865.
[13] Burr, J.G., Dreyfuss, G., Penman, S. and Buchanan, J. M. (1980) Proc. Natl. Acad. Sci. USA 77, 3484–3488.
[14] Moriyama, Y. and Nelson, N. (1989) J. Biol. Chem. 264, 3577–3582.
[15] Väänänen, H.K. (1984) Histochemistry 81, 485–487.
[16] Moriyama, Y., Maeda, M. and Futai, M. (1990) J. Biochem. 108, 689–693.
[17] Ito, K., Kobayashi, T., Moriyama, Y., Toshima, K., Tatsuya, K., Kaiuchi, T., Futai, M., Ploegh, H., and Miwa, K. (1995) J. Antibiot. 48, 488–494.
[18] Sasaki, T., Hong, M.H., Udagawa, N., and Moriyama, Y. (1994) Cell Tissue Res. 278, 265–271.
[19] Beier, D.R., Dushkin, H., Her, H. and Brady, K.P. (1996) Mouse Molecular Genetics, abstr., pp. 327.